

## Enhanced photothermal lens using a photonic crystal surface

Yunfei Zhao,<sup>1</sup> Longju Liu,<sup>1</sup> Xiangwei Zhao,<sup>2</sup> and Meng Lu<sup>1,3,a)</sup>

<sup>1</sup>Department of Electrical and Computer Engineering, 2128 Coover Hall, Iowa State University, Ames, Iowa 50011, USA

<sup>2</sup>State Key Laboratory of Bioelectronics, School of Biological Science and Medical Engineering, Southeast University, Nanjing, Jiangsu 211189, People's Republic of China

<sup>3</sup>Department of Mechanical Engineering, Iowa State University, Ames, Iowa 50011, USA

(Received 21 June 2016; accepted 8 August 2016; published online 17 August 2016)

A photonic crystal (PC)-enhanced photothermal lens (PTL) is demonstrated for the detection of optically thin light absorption materials. The PC-enhanced PTL system is based on a pump-probe scheme consisting of a PC surface, pump laser beam, and probe laser beam. Heated by the pump beam, light absorption materials on the PC surface generate the PTL and cause a substantial change to the guided-mode resonance supported by the PC structure. The change of the PC resonance is detected using the probe laser beam by measuring its reflectivity from the PC surface. When applied to analyze dye molecules deposited on the PC substrate, the developed system is capable of enhancing the PTL signal by 10-fold and reducing the lowest distinguishable concentration by 8-fold, in comparison to measuring without utilizing the PC resonance. The PC-enhanced PTL was also used to detect gold nanoparticles on the PC surface and exhibited a 20-fold improvement of the lowest distinguishable concentration. The PC-enhanced PTL technology offers a potential tool to obtain the absorption signatures of thin films in a broad spectral range with high sensitivity and inexpensive instrumentation. As a result, this technology will enable a broad range of applications of photothermal spectroscopy in chemical analysis and biomolecule sensing. *Published by AIP Publishing.*  
[\[http://dx.doi.org/10.1063/1.4961376\]](http://dx.doi.org/10.1063/1.4961376)

Photothermal spectroscopy indirectly measures the sample absorbance through the detection of heat generation by samples.<sup>1,2</sup> The photothermal techniques are highly sensitive when applied to quantitative determination of the sample absorption.<sup>3</sup> Several photothermal-based methods, such as photothermal lens (PTL)<sup>4,5</sup> and photothermal deflection,<sup>6–8</sup> have been implemented for chemical analysis, microscopic study of nanoparticles, biomolecule sensors, etc.<sup>9–12</sup> As an analytic method, photothermal spectroscopy offers several important features for chemical analysis. For example, material absorption in the UV, visible, IR, and THz ranges can all be measured with minimum modifications of the detector. In addition, the sample quantification can be performed over a substantial range of concentrations. In order to characterize optically thin samples, detection apparatuses, such as the attenuated total reflection,<sup>13</sup> optical cavities,<sup>14,15</sup> and micro-mechanical devices,<sup>16</sup> have been demonstrated. Here, to improve the sensitivity of PTL detection, a one-dimensional photonic crystal (PC) surface is exploited to magnify the change of the probe beam and results in stronger PTL signals.

The PC slab, comprised of a nanostructured dielectric thin film, supports a guided-mode resonance.<sup>17–19</sup> When the PC surface is excited under resonance conditions, it exhibits narrowband optical resonances with intensified local fields. Several applications of PC-based devices have been demonstrated for optical filters, refractometric sensors, and fluorescence-based biosensors.<sup>20–24</sup> Here, the PC surface is exploited to enhance the PTL for two main reasons. First, the PC structure can be engineered to exhibit the resonant

wavelength from visible to mid-infrared,<sup>25</sup> and thus the resonant wavelength can be easily matched to the light beams used in the PTL system. Second, it is inexpensive to fabricate PC structures over a large surface area using plastic materials with low thermal conductivity.<sup>26</sup> Our previous work has shown the PC-enhanced photoacoustic phenomena based on the strong near field of the PC resonance.<sup>27</sup>

This letter reports the PC-enhanced PTL effect that is characterized using a pump-probe scheme. The light absorbing material coated on the PC substrate is heated by the pump beam and generates the thermal lens, which is monitored by the probe laser beam at a different wavelength. The PC surface enhances the PTL signal via the following mechanisms. When the pump laser is turned off, we adjust the incident angle of the probe beam to couple it into a PC resonance mode. The reflection resonance allows the PC surface to reflect the probe beam with a high reflectivity ( $R$ ). If the pump laser is turned on, the absorption of the pump laser creates a thermal gradient adjacent to the sample surface. The light-induced heat produces a refractive index profile in air that functions as the thermal lens to deflect the probe beam.<sup>8</sup> As a result, the probe beam is no longer coupled with the PC resonance and the reflectivity decreases. In the meantime, the light-induced heat also causes a spectral shift of the PC resonance and reduces the reflectivity. The shift can be associated with the refractive index change of air, sample, and PC surface, as well as the physical expansion of the grating structure. The combination of the thermal lens deflection and resonance shift gives rise to the PC-enhanced PTL phenomenon. The PC enhancement magnifies the change of reflectivity ( $\Delta R$ ) relative to an un-patterned surface. In this paper, two PTL experiments are carried out to demonstrate the

<sup>a)</sup>Electronic mail: menglu@iastate.edu

PC-enhanced PTL analysis of organic dye molecules and metal nanoparticles.

In the PTL setup shown in Fig. 1, the pump laser (85-RCA-400, Melles Griot) emits at  $\lambda_{\text{pump}} = 660$  nm with the power of  $P_{\text{pump}} = 240$  mW. The pump beam is focused on the PC by a convex lens ( $f = 50$  mm). A probe laser (MingNuo OpticElectronic Co. Ltd.) with  $\lambda_{\text{probe}} = 532$  nm and  $P_{\text{probe}} = 5$  mW is used to detect the pump-induced changes around the PC surface. The probe beam is reflected by the mirror (M1) and polarized by the linear polarizer. The incident angle of the probe laser beam is precisely tuned by translating the M1 using a linear translation stage (PT1B, Thorlabs Inc.) to couple it efficiently into a PC resonance mode. The reflected probe beam from the PC passes through a bandpass filter ( $\lambda_c = 532$  nm and  $\Delta\lambda = 5$  nm) and an aperture (diameter of 2 mm) before hitting the photodetector (PDA10A, Thorlabs Inc.). The output of the photodetector was measured using an oscilloscope (TDS2014B, Tektronix). During a test, the pump beam was switched on and off using the chopper. The measurements were taken 3 s after the switching of the pump beam to allow the sample to reach a stabilized thermal state. The differences of the reflectance ( $\Delta R/R$ ) under these two circumstances (on and off) were recorded as the PTL signal.

The cross-sectional view of the PC structure used for the PTL measurement is shown in Fig. 1. The PC is based on a surface relief grating with a period of  $\Lambda = 400$  nm, a duty cycle of 60%, and a depth of 80 nm. The sub-wavelength grating pattern was fabricated using a single-step, high-throughput, and inexpensive nanoreplica molding process.<sup>28</sup> This process used a liquid ultra-violet curable epoxy (NOA88, Norland Products, Inc.) squeezed between the silicon mold and a transparent plastic film. The silicon mold carried a negative grating pattern and was fabricated

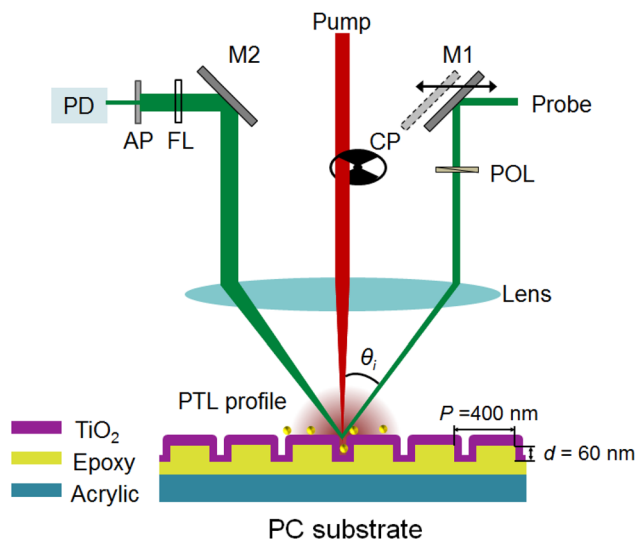


FIG. 1. Concept of the PC-enhanced PTL system. The schematic plot is not to scale. In the experiments, the PC sample is simultaneously illuminated with the pump beam at 660 nm and the probe beam at 532 nm. The pump beam is turned on and off by a chopper (CP) and focused on to the PC surface. The thermal lens generated by the AuNPs is shown as the PTL profile. The probe laser is polarized by the linear polarizer (POL) and the incident angle is tuned by translating the mirror (M1). The reflected beam passes through the same focusing lens and is directed towards the photodetector (PD) through the mirror (M2), the laser line filter (FL), and the aperture (AP).

using an electron-beam lithography process followed by a reactive ion etching. After the liquid epoxy was cured using UV light, the substrate was peeled off from the silicon mold. To complete the fabrication of the PC, a high refractive index dielectric thin film, i.e., the 85-nm-thick  $\text{TiO}_2$  layer, was deposited using an e-beam evaporator (Temescal). The grating substrate was composed of polymer materials with low thermal conductivity to benefit the generation of PTL. As the waveguide layer of the PC resonator, an 85-nm-thick  $\text{TiO}_2$  thin film (refractive index,  $n = 2.2$ ) was coated on the grating surface. The PC device was carefully designed to maximize the strength of the optical resonance when it was excited by the probe laser beam at  $\lambda_{\text{probe}} = 532$  nm. The PTL detections of two different types of test samples, including a light absorbing organic dye and gold nanoparticles (AuNPs), were performed. The organic dye samples (Epolight 6661, Epolin Inc) were dissolved in ethanol and spin coated on the PC. The AuNPs (Nanopartz C12-10-700) were suspended in the buffer solution and drop-cast on the PC substrate.

The resonant modes of the PC can be excited by a plane wave at a particular coupling incidence ( $\theta_i$ ) and resonant wavelength ( $\lambda_r$ ). Previous studies have demonstrated that the PC resonances can result in narrowband peaks in the reflection spectrum. Therefore, to identify the PC resonances for the PTL measurement, we numerically and experimentally characterize the reflection spectra of the fabricated PC. The numerical study is based on the rigorous coupled-wave analysis (DiffractMod, Synopsis) that aids the design and testing of the PC. The simulation region was setup to the unit volume of the periodic structures. Periodic boundary conditions were applied to truncate the calculation domain in the grating plane. Ten spatial harmonics were used to represent the device and fields in the computational domain. The refractive indexes of  $\text{TiO}_2$  and epoxy are 2.2 and 1.47, respectively. The incident wave was transverse magnetic (TM) polarized. Reflection spectra of the PC structure were calculated in the wavelength range from 450 nm to 750 nm when the incidence angle was  $0^\circ$ . The calculated reflection spectrum of the aforementioned PC structure with an incident angle of  $\theta_i = 12^\circ$  is plotted in Fig. 2 as a blue curve. The spectrum exhibits two distinct PC resonant peaks at  $\lambda_r = 527$  nm and 645 nm. The experimental characterization was conducted by measuring the reflection spectrum of the PC surface by tuning the incident angle to obtain a narrowband resonance near 532 nm. The PC devices support both transverse magnetic (TM) and transverse electric (TE) modes, with the electric field components perpendicular and parallel to the grating, respectively. In this work, we use the TM-polarized resonance to reflect the probe beam. A polarizer is used to control the polarization of the incident or probe beam. Tuning the incident angle allows the excitation of a resonance mode that spectrally overlaps the probe laser at  $\lambda_{\text{probe}} = 532$  nm through the phase matching from the PC. The reflection spectrum measured at  $\theta_i = 12^\circ$  is shown as the black curve in Fig. 2. The measured spectrum matches well with the computer-simulated spectrum. The spectral position of the pump and probe laser beams is labeled in Fig. 2 using the green and red lines, respectively. In the absence of the heating effect, the resonance at  $\lambda_r = 532$  nm can effectively

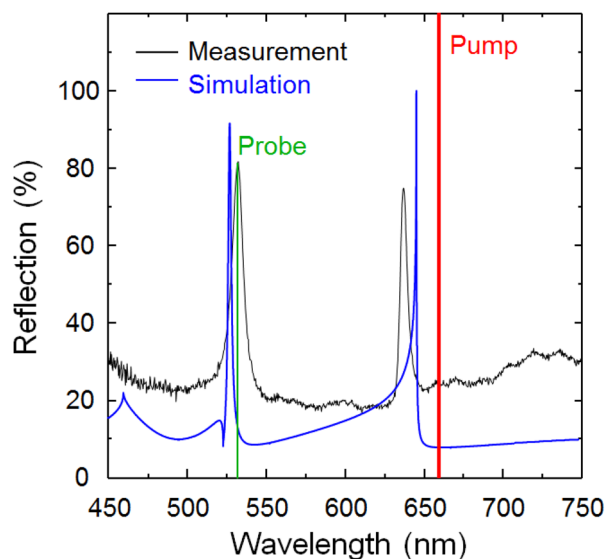


FIG. 2. Characterizations of the PC sample. The simulation and experimental result of the PC reflection spectrum when  $\theta_i = 12^\circ$ . The spectral locations of the probe and pump laser beams are represented by the green and red lines, respectively. The probe beam is coupled to the PC resonance at 532 nm, but the pump laser does not overlap with any PC resonance.

reflect the probe beam. The Q-factor of this resonance mode is approximately 66. It is worth noting that when the pump beam ( $\lambda_{\text{pump}} = 660 \text{ nm}$ ) is focused normal to the PC surface, it is not coupled with any PC resonance mode.

In order to characterize the PC-enhanced PTL effect, we investigated the PTL signals of a light absorbing dye molecule that absorbs strongly in the wavelength range of 600 nm to 700 nm with the absorption peak located at 666 nm. The dye was coated on the PC surface at a concentration of 1.0 mg/ml to absorb the pump beam. Fig. 3(a) shows the pictures of the reflected probe beam spots when the pump beam was off (left panel) and on (right panel). A significant light intensity change occurs at the center of the probe beam spot when the absorbed pump energy heats the surrounding air. The region of hot air has a lower refractive index and acts as a thermal lens to diverge the probe beam. The thermal lens also causes the shift of the PC resonance and reduces the reflectivity of the probe beam. The reflected probe beam is masked using an aperture that only allows the region circled in red (Fig. 3(a)) to pass through. The light intensity change ( $\Delta R$ ) within this particular region is monitored using the photodetector. The change in reflectivity ( $\Delta R/R$ ) is calculated as the PTL signal. Fig. 3(a) clearly shows that the presence of PTL decreases the reflection of the probe beam by the PC surface. Fig. 3(b) shows the measurement of the PTL signal as a function of the incident angle. The transmission of the probe laser beam through the PC is also plotted in Fig. 3(b) to confirm the effect of the PC resonance. For the transmission measurement, the PC was mounted a rotation stage. The probe laser beam (532 nm) was polarized using the linear polarizer and passed through the PC substrate. By rotating the PC, the incident angle was tuned from  $4^\circ$  to  $16^\circ$  with the incremental of  $1^\circ$ , and  $0.5^\circ$  near the resonance peak. The transmitted laser beam was measured using a photodiode (PDA10A, Thorlabs Inc.). The transmittance was calculated as the measured power divided by the output power of the

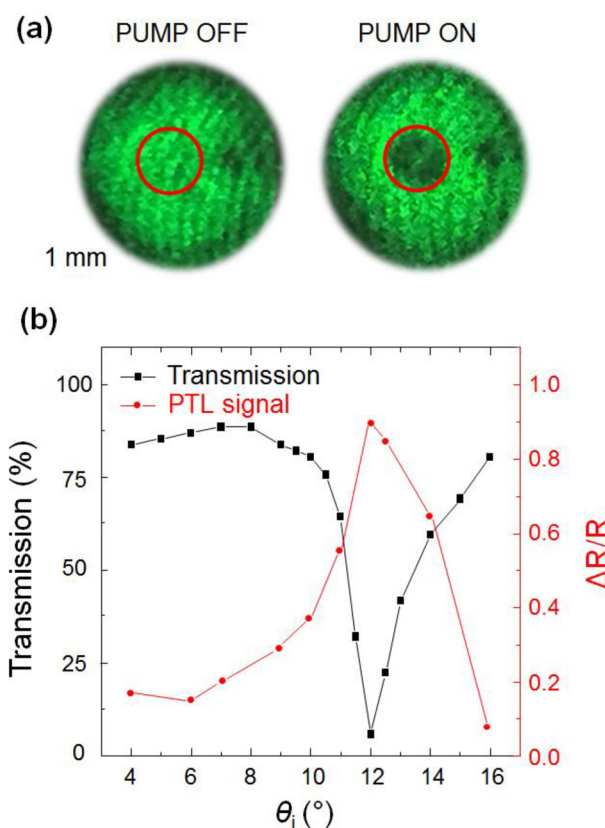


FIG. 3. Measurements of the PTL signal. (a) Photographs of the reflected probe beam taken when the pump laser beam is switched off (left panel) and on (right panel). (b) Transmission of the probe laser through the PC substrate and the PTL signals. Both curves were measured as a function of the incident angle of the probe beam.

probe laser (5 mW). In the transmission curve, the dip that represents the PC resonance appears at  $\theta_i = 12^\circ$ . The peak value of the PTL signal occurs at the same angle, and the PTL signal well correlates with the PC resonance. The PTL signal measured at  $\theta_i = 12^\circ$  (on-resonance) is 10-fold higher than the signal at  $\theta_i = 16^\circ$  (off-resonance).

Furthermore, Fig. 4 shows the PTL results of a titer of the dye sample using a 2-fold dilution series with a total of eight concentrations in the range of  $8.0 \mu\text{g/ml}$  to  $1.0 \text{ mg/ml}$ . For each concentration, a  $20\text{-}\mu\text{l}$  droplet was pipetted onto the same PC with three duplicated spots. After drying under the ambient condition for 20 min, the samples were ready for the PTL test. In Fig. 4, the black curve represents the PTL signals measured under the resonance condition, where the probe laser was coupled into the PC resonance mode at  $\theta_i = 12^\circ$ . As a reference, the red curve in Fig. 4 shows the PTL results with the probe beam uncoupled with the PC resonance mode. The PTL signals measured on-resonance are significantly higher than the off-resonance signals. The PC resonance effectively improves the linear detection range. The key performance metrics for PTL analysis is the limit of detection at the lowest distinguishable concentration of the dye. As shown in Fig. 4, the limit of detection for the on-resonance measurement is  $0.031 \text{ mg/ml}$ , whereas the limit of detection for the off-resonance measurement is  $0.25 \text{ mg/ml}$ . Therefore, the PC resonance offers a sensitivity enhancement by a factor of 8. It is worth noting that the curve for the on-resonance PTL signal saturated at  $1 \text{ mg/ml}$  due to

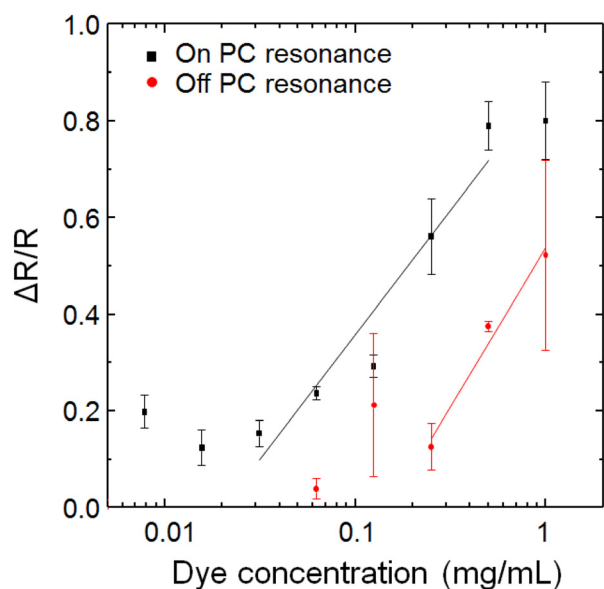
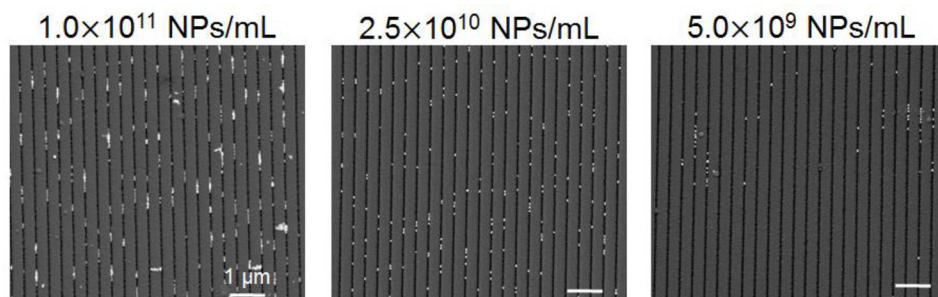


FIG. 4. PTL measurement of light absorbing dye. The black and red curves correspond to the tests with the probe laser coupled to PC resonance at  $\theta_i = 12^\circ$  and off the PC resonance ( $\theta_i = 24^\circ$ ), respectively. The linear range of each measurement was fitted using a linear curve.

deterioration of the Q-factor of the PC caused by excessive amount of organic dye.

Having demonstrated the PTL signal enhancement of the PC surface to the organic light-absorbing molecules, we next exploited the PC-enhanced PTL for the analysis of gold nanoparticles (AuNPs). A dilution series was made that contained the following concentrations (in NPs/ml):  $2.5 \times 10^{11}$ ,  $1.0 \times 10^{11}$ ,  $5.0 \times 10^{10}$ ,  $2.5 \times 10^{10}$ ,  $1.0 \times 10^{10}$ ,  $5.0 \times 10^9$ ,  $2.5 \times 10^9$ ,  $1.0 \times 10^9$ , and  $5.0 \times 10^8$ . For each concentration, a 20- $\mu$ l droplet was pipetted onto the same PC surface with three duplicated spots. After drying under the ambient condition for one hour, the samples were ready for the PTL measurement. Figure 5(a) shows the SEM images of the AuNP coated PC substrates with AuNP concentrations of  $1.0 \times 10^{11}$ ,  $2.5 \times 10^{10}$ , and  $5.0 \times 10^9$  NPs/ml. The PC was not only capable of increasing the PTL signals substantially but also capable of reducing the detection limit significantly. To validate this hypothesis, PC samples with AuNPs in a range of concentrations from  $5.0 \times 10^8$  NPs/ml to  $2.5 \times 10^{11}$  NPs/ml were measured when the PC was illuminated on-resonance ( $\theta_i = 12^\circ$ ) and off-resonance ( $\theta_i = 24^\circ$ ). The PTL signals measured under on-resonance and off-resonance conditions are compared in Fig. 5(b). The PC resonance enabled

(a)



(b)

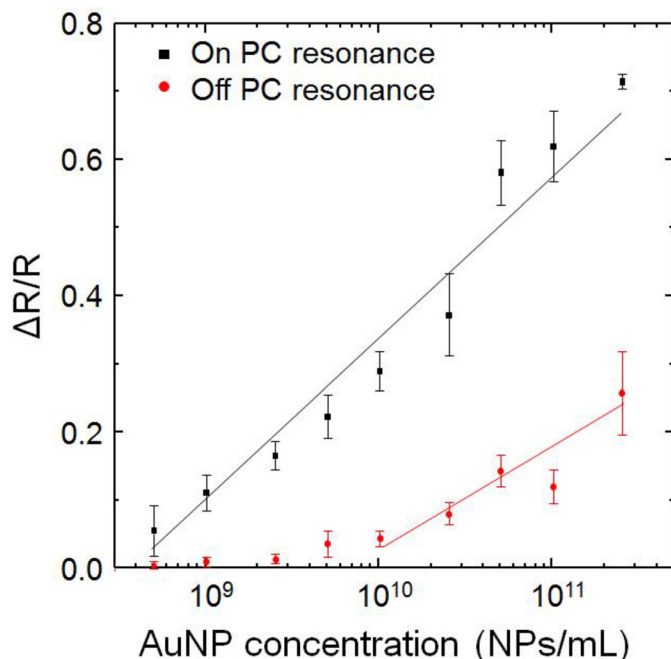


FIG. 5. Measurements of AuNPs. (a) SEM images of AuNPs dispersed on PC surfaces at three different concentrations. (b) PTL signals of AuNPs plotted as a function of the AuNP concentration. The black and red curves correspond to the tests with the probe laser coupled to PC resonance ( $\theta_r = 12^\circ$ ) and off the PC resonance ( $\theta_i = 24^\circ$ ), respectively. The linear range of each measurement was fitted using a linear curve.

the detection of AuNPs with a concentration as low as  $5.0 \times 10^8$  NPs/ml, which represented a 20 times lower detection limit with regard to the off-resonance analysis. Moreover, the on-resonance measurement exhibits a larger dynamic range than the off-resonance measurement. As shown in Fig. 5(b), the curve measured with the PC resonance shows a linear response range of  $5 \times 10^8$  NPs/ml to  $2.5 \times 10^{11}$  NPs/ml, whereas the linear range of the off-resonance measurement only ranges from  $1.0 \times 10^{10}$  NPs/ml to  $2.5 \times 10^{11}$  NPs/ml. Therefore, the PC-enhanced PTL is suitable for measuring AuNPs with a greater detection sensitivity and a broader dynamic range.

In summary, a 1D PC surface has been applied to enhance the PTL detection of light absorbing materials deposited on the PC surface. Based on the pump-probe setup, our results show that the resonant reflection of the PC surface can boost the change of the PTL signal. During the tests, the PC surface was designed and fabricated to reflect the probe laser beam effectively. In the presence of the optically thin absorbing sample, the pump beam-induced thermal lens causes the shift of the PC resonance and consequently reduces the reflectance of the probe laser beam. The PC-enhanced PTL approach was tested using the light absorbing dye and AuNPs. For the measurement of the dye molecules, a signal enhancement over ten times is observed when the probe laser is coupled with the PC resonance, as compared to not utilizing the PC resonance. The PC-enhanced PTL effect significantly reduces the detection limit of dye molecules and AuNPs by factors of 8 and 20, respectively.

The PC-enhanced PTL system demonstrated in this work is to set an example of using PC resonance to enhance the pump-probe analysis of optically thin materials. While this PC design is adequate in demonstrating the enhancement effect, the PC performance may be optimized further with regard to the PTL signal. For example, the measured linewidth of the PC resonance is 7.3 nm, and previous studies have shown that engineering the geometry of the PC structure can effectively reduce the resonance linewidth.<sup>29</sup> A PC resonance with a narrower linewidth will enable a more prominent change in the reflectance of the probe beam, and thus, improve the sensitivity to the thermal lens. The PTL signal can be further enhanced by coupling both pump and probe beams into different resonant modes of the PC surface. Like the double resonance PC nanobeam sensor theoretically studied by Lin *et al.*,<sup>30</sup> the PC surface can also improve the absorption of molecules when the PC resonance, pump beam, and molecule absorption spectrally overlap.

The PC-enhanced PTL technology is not limited to the laser-induced PTL but can also be applied to broadband light pumped systems for the measurement of the absorption spectra of unknown samples. Integrated with a Fourier transform infrared spectrometer, which is an essential tool for chemical analysis based on absorption signatures, the PC-enhanced PTL can indirectly detect the infrared absorption of optically thin samples and has the potential to offer an enhanced

sensitivity. In future work, this technique will also be exploited to facilitate the photothermal detection of disease biomarkers.<sup>31</sup>

This research was supported by the start-up funding from the Iowa State University and the 3M Non-Tenured Faculty Award. The authors would like to thank Dr. John F. McClelland of MTEC Photoacoustics Inc. for the valuable discussions.

- <sup>1</sup>H. Coufal, *Fresen J. Anal. Chem.* **337**, 835 (1990).
- <sup>2</sup>L. A. Skvortsov, *Quantum Electron.* **43**, 1 (2013).
- <sup>3</sup>S. Bialkowski, *Photothermal Spectroscopy Methods for Chemical Analysis* (Wiley, New York, USA, 1996).
- <sup>4</sup>A. V. Brusnichkin, D. A. Nedosekin, M. A. Proskurnin, and V. P. Zharov, *Appl. Spectrosc.* **61**, 1191 (2007).
- <sup>5</sup>R. D. Snook and R. D. Lowe, *Analyst* **120**, 2051–2068 (1995).
- <sup>6</sup>A. C. Boccara, D. Fournier, W. Jackson, and N. M. Amer, *Opt. Lett.* **5**, 377 (1980).
- <sup>7</sup>W. B. Jackson, N. M. Amer, A. C. Boccara, and D. Fournier, *Appl. Opt.* **20**, 1333 (1981).
- <sup>8</sup>A. C. Boccara, D. Fournier, and J. Badoz, *Appl. Phys. Lett.* **36**, 130 (1980).
- <sup>9</sup>D. Boyer, P. Tamarat, A. Maali, B. Lounis, and M. Orrit, *Science* **297**, 1160 (2002).
- <sup>10</sup>A. Gaiduk, P. V. Ruijgrok, M. Yorulmaz, and M. Orrit, *Chem. Sci.* **1**, 343 (2010).
- <sup>11</sup>Y. Li and R. Gupta, *Appl. Opt.* **42**, 4396 (2003).
- <sup>12</sup>S. J. Lu, W. Min, S. S. Chong, G. R. Holtom, and X. S. Xie, *Appl. Phys. Lett.* **96**, 113701 (2010).
- <sup>13</sup>T. Shimosaka, T. Sugii, T. Hobo, J. B. A. Ross, and K. Uchiyama, *Anal. Chem.* **72**, 3532 (2000).
- <sup>14</sup>S. Horita, E. Miyagoshi, M. Ishimaru, and T. Hata, *Rev. Sci. Instrum.* **63**, 1909 (1992).
- <sup>15</sup>H. A. Schuessler, S. H. Chen, Z. Rong, Z. C. Tang, and E. C. Benck, *Appl. Opt.* **31**, 2669 (1992).
- <sup>16</sup>J. R. Barnes, R. J. Stephenson, M. E. Welland, C. Gerber, and J. K. Gimzewski, *Nature* **372**, 79 (1994).
- <sup>17</sup>S. S. Wang, R. Magnusson, J. S. Bagby, and M. G. Moharam, *J. Opt. Soc. Am. A* **7**, 1470 (1990).
- <sup>18</sup>Y. Ding and R. Magnusson, *Opt. Express* **12**, 1885 (2004).
- <sup>19</sup>S. H. Fan and J. D. Joannopoulos, *Phys. Rev. B* **65**, 235112 (2002).
- <sup>20</sup>M. J. Uddin and R. Magnusson, *IEEE Photonics Tech. Lett.* **24**, 1552 (2012).
- <sup>21</sup>D. Wawro, S. Tibuleac, R. Magnusson, and H. Liu, *Proc. SPIE.* **3911**, 86 (2000).
- <sup>22</sup>C. S. Huang, S. George, M. Lu, V. Chaudhery, R. M. Tan, R. C. Zangar, and B. T. Cunningham, *Anal. Chem.* **83**, 1425 (2011).
- <sup>23</sup>B. Cunningham, P. Li, B. Lin, and J. Pepper, *Sens. Actuators, B* **81**, 316 (2002).
- <sup>24</sup>Y. Zhuo, H. Hu, W. L. Chen, M. Lu, L. M. Tian, H. J. Yu, K. D. Long, E. Chow, W. P. King, S. Singamaneni, and B. T. Cunningham, *Analyst* **139**, 1007 (2014).
- <sup>25</sup>J. N. Liu, M. V. Schulmerich, R. Bhargava, and B. T. Cunningham, *Opt. Express* **22**, 18142 (2014).
- <sup>26</sup>V. Chaudhery, S. George, M. Lu, A. Pokhriyal, and B. T. Cunningham, *Sensors* **13**, 5561 (2013).
- <sup>27</sup>Y. F. Zhao, K. Y. Liu, J. McClelland, and M. Lu, *Appl. Phys. Lett.* **104**, 161110 (2014).
- <sup>28</sup>C. Ge, M. Lu, X. Jian, Y. F. Tan, and B. T. Cunningham, *Opt. Express* **18**, 12980 (2010).
- <sup>29</sup>I. D. Block, N. Ganesh, M. Lu, and B. T. Cunningham, *IEEE Sens. J.* **8**, 274 (2008).
- <sup>30</sup>H. Lin, Z. Yi, and J. Hu, *Opt. Lett.* **37**, 1304–1306 (2012).
- <sup>31</sup>Y. Zhao, M. Cao, J. F. McClelland, Z. Shao, and M. Lu, *Biosens. Bioelectron.* **85**, 261 (2016).